International Journal of ISSI, Vol.12 (2015), No.1, pp. 1-8

Evaluation of Microstructure and Wear Behavior of Iron-based Hard - facing Coatings on the Mo40 Steel

K. Amini [1]*, A. Bahrami [2], H. Sabet [3]

[1] *Department of Mechanical Engineering, Tiran Branch, Islamic Azad University, Isfahan , Iran*
[2] *Department of Materials Engineering, Najaf Abad Branch, Islamic Azad University, Isfahan , Iran*
[3] *Department of Materials Engineering, Karaj Branch, Islamic Azad University, Karaj , Iran*

Abstract

Mo40 low-alloy steels are mostly used to produce industrial components such as crane wheels which are exposed to abrasive wear. However, during working conditions, their wear resistance is reduced after a while due to its low hardness. With increasing abrasive wear, the dimensions of components decrease and they need to be repaired for surface modification. In this regard, hard overlay coatings are applied by hard-facing process for reusing these components. This work deals with the surface analysis, hardness and wear behaviors of the clad layers made of the Fe-Cr-C based hard-facing on the Mo40 low-alloy steel by submerged arc welding method. The overlay coatings are performed by two ways of welding: 1. rods of UP6-GF-50 (307 kavosh joosh standard number), and 2. UP6-GF-50-C (420 kavosh joosh standard number) regarding the Din 8555 standard, in single and double passes. According to the X-ray diffraction analysis and microstructure characteristics, both martensite with retained austenite phases and the (Fe, Cr)23 C6 carbides were identified within the overlay coatings. The presence of the carbon and chromium elements in hard surfaced specimens (as denoted by 307 and 420) produced by single and double pass were increased. The wear resistance in the coatings of 307 and 420 produced by double pass are higher than the coatings produced by single pass. In addition, the amount of average hardness in the coatings of 307 and 420 produced by single and double passes increases from 36 to 38 HRC and from 39 to 42 HRC, respectively. Based on the scanning electron microscopy micrographs, the wear mechanisms of specimens with high hardness are adhesive and tribochemical wear.

Keywords: Mo40 steel, Submerged arc welding, Coating, Hard-facing, Wear resistance.

1. Introduction

Hard-facing is a modern surface welding method in which an almost thick layer of metal with hard intermetallic phases such as carbides is deposited on the surface of industrial components by means of welding, spraying, and other methods. This technique was invented by Winston and sherlley in 1921 and has been quickly developed because of its high capacity in cladding by dissimilar welding and joining processes.

Another advantage of this cladding method concerns the ability of components to supply the rather contradictory properties in one part simultaneously.

For instance, some properties such as brittleness and ductility in the substrate and hardness in the overlay coating can be created. In addition, this process is highly efficient [1)]. Nowadays, hard-facing method has been widely used for repairing and resurfacing of components in shipbuilding, rail-way transportation, and heavy industries.

Basically, hard-facing by welding method can be divided into two main classifications including solid-state cladding and fusion cladding. The properties of hard overlay coatings depend on chemical composition, solidification conditions, cooling rate after solidification, microstructure, type, shape, and distribution of the hard phase precipitates [2-3)]. Two kinds of alloys are mainly used for creation of wear resistance overlay coatings on iron-based alloys (i.e. carbon steel, and low-alloy steel) [4)]. They include ferrous and non-ferrous alloys which can be categorized into the Fe-Cr-C based and the Fe-C-X based alloys. One of the common methods for surface modification involves adding the alloy elements such as chromium, carbon, cobalt, molybdenum or ceramic particles including SiC, TiC, WC, and B_4C into the melting region on the surface and producing overlay coating with considerable thickness on the surface of components [5, 6)].

* *Corresponding Author*
Tell: +98 335 545 2290-4
Email: K_amini@iautiran.ac.ir
Address: Department of Mechanical Engineering, Tiran Branch, Islamic Azad University, Isfahan , Iran
1. Assistant Professor
2. Assistant Professor
3. M.Sc.

For example, Lin et al. [7] researched on the analysis of microstructure and wear performance of the SiC clad layer on the SKD61 die steel after gas tungsten arc welding. They reported that the SiC powder had been almost decomposed into the stable and meta-stable phases and it caused the increase of hardness and wear resistance in the surface-clad layer. Similarly, Yuan et al. [8] also cladded the TiC powder on the surface of Ti_6Al_4V alloy by gas tungsten arc welding (TIG) with flux core rod. They stated that in this method, a good metallurgical bonding can be obtained between the substrate and the overlay coating. Buytoz et al. [9] studied on the surface cladding of the AISI 304 stainless steel with SiC particles by TIG surface alloying.

They showed that with decreasing the heat input and increasing the SiC content of the powder, the amount of dilution reduced to minimum. Soodi et al. [10] studied the effect of the laser cladding process on the integrity of metal substrates of 420 stainless steel, the bond between the cladding and base metal, and physical characteristics of the cladding layer. They concluded that, due to the small size of the heat-affected zone, the laser cladding process does not adversely affect the physical properties of the metallic substrates. Additionally, Vukvoic et al. [11] evaluated the effective parameters on re-hard surfacing of steel R7T wheel train wagons in order to improve the wear resistance.

They presented that with controlling the cooling rate of weld deposition and considering the sufficient pre-heating temperature in resurfacing of wheels, mechanical and metallurgical properties of weld metal can be meliorated. This study focuses on hard facing of the Mo40 steels. These steels are regularly used as the rolling rollers in the steel companies. This kind of roller is vastly used in the Foulad Mobarakeh Company and is repaired via this method. The hardness of the steel is improved after repair and the roller is used again in service after the repaired. Thus, the aim of this research to evaluate and compare the microstructure, hardness, wear resistance, as well as lifetime of the overlay coatings which are deposited by two kinds of flux core rods such as 307 and 420 (Kavosh Joosh Company (Iran) standard number). In addition, it is aimed to select the suitable rod for cladding of Mo40 steel to increase the wear resistance.

2. Experimental Details

In this study, four classes of Mo40 low-alloy steel were prepared into 12 × 290 × 300 mm specimens as welding substrates. Before welding, the specimens were grinded and cleaned with acetone. Nominal chemical composition of the substrate is presented in Table 1. Hard overlay coatings were produced by submerged arc welding (SAW) technique on flat low-alloy steel specimens. Table 2 shows the welding conditions used in this research. The SAW weld deposition parameters are listed in Table 3. In addition, the nominal composition of the material used to perform overlay coatings are presented in Table 4. Optical emission spectroscopy (OES) was used for identification of chemical composition of the coatings according to ASTM 415 in three different points of the coating surfaces. In order to evaluate microstructure of the substrate as a base metal and the overlay coating, the surface of the specimens was prepared by polishing and etching. The Nital solution (5%) was selected as an etching agent. After surface preparation of the specimens, microstructure investigations were performed by optical microscopy (OM), scanning electron microscopy (SEM), and energy dispersive X-ray (EDS) spectroscopy. The carbides were clarified and colored during etching. Then, their percentage was calculated via Clemex Vision (version 3.5.025) image analysis software. The volume fraction of the hard phases was measured by means of the qualitative metallography method and micrograph J software.

The presences of the phases within overlay coatings were identified by x-ray diffraction (XRD) after surface alloying with the SAW process. The Cu-Kα generated at 20 KV and 30 mA was used as a radiation source. The hardness values (HRC) were measured on the top surface of the overlay coatings.

Each hardness measurement was done at least three times to obtain the average hardness. According to ASTM G9912), the wear resistance was evaluated using a pin-on-disk rotating type tribometer. The wear test parameters are listed in Table 5. An upper moving specimen, the pin, was made of the hardened AISI 52100 bearing steel. The wear test specimen was cut by wire EDM machine in cylindrical shape with 50 mm diameter and 5 to 10 mm thicknesses and used as a disk counter specimen. Finally, the mass loss was measured by balance with 0.0001 g precision. For load selection the samples were tested in different loads in the distance of 100m.

After the 100 meter sliding distance the samples weight were evaluated using a digital balance with the accuracy of 0.001 gram. The load in which the weight lose being severely visible was chosen as the wear test load and the test were performed in that load. Each test was repeated at least for two times and the average value of the weight loss and wear rate was reported.

Table 1. Chemical composition of low-alloy steel of Mo40 used in this research.

C	Si	Mn	P	S	Cr	Mo	Ni	V	Fe	Element
0.38	0.21	0.69	0.0035	0.0016	0.96	0.2	0.03	0.004	Bal.	wt.%

Table 2. Process parameters of hard-facing in the SAW method.

Thickness of cladding (mm)	No. pass	Type of Flux (DIN 35522 standard)	Type of wire (DIN 8555 standard)	Wire code (Kavosh Joosh standard number)
4	1	Flux in Flux out B AB 1 68 AC	UP6-GF-50	307
7	2			
4	1	Flux in Flux out B FB 1 55 AC	UP6-GF-50-C	420
7	2			

Table 3. Specifications of the hard-facing specimens.

Post-heating (°C)	Pre-heating (°C)	Current (A)	Voltage (V)	Arc length (mm)	Wire diameter (mm)	Welding speed (cm/min)	polarity	NO. Passes	process
Max.100	200-250	40-45	28-30	2.5-3.5	3.2	60-70	DCEP	1&2	SAW

Table 4. Chemical composition of wires and powders used in this research.

Material	C	Si	Mn	Cr	Ni	Mo
Wire 307	0.24-0.26	0.6-0.9	1.8-1.9	4-4.5	Max.0.2	0.8-1
Wire 420	0.25-0.35	0.3-0.5	0.5-0.7	12-14	-	-
Powder 610	0.04-0.07	0.3-0.4	1.4-1.6	1-1.2	-	-
Powder 915	0.04-0.07	0.6-0.8	0.7-0.9	1.1-1.2	1.8-2	0.45-0.55

Table 5. The wear test conditions.

Sliding conditions	Dry sliding conditions
Load (N)	130
Sliding speed (ms^{-1})	0.05
Sliding distance (m)	1000
Temperature	Room temperature

3. Results and Discussion

3.1. Chemical analysis

The chemical composition of the overlay coatings are presented in Table 6. As can be seen, chemical composition of overlay coatings produced by double pass is changed as opposed to those produced by single pass. The changing in chemical composition can be a result of the amount of dilution of the base metal during the cladding process. Accordingly, the presence of elements in base metal decreases at overlay coating with increasing the number of passes. Based on Table 6, it is obvious that the presence of the carbon and chromium elements in hard surfaced specimen (as denoted by 307) produced by single and double passes increases from 0.28 to 0.32 and from 3.54 to 4.10, respectively. This is to say that the volume fraction of the hard phases changes with increasing the weight percent of these effective elements. The obtained results from this research are in good agreement with the results reported by other researchers [13].

Table 6. Chemical composition of created coating (wt.%).

Type of coating	C	Si	Mn	Cr	Ni	Mo	V	Fe
Single pass- 307	0.28	0.53	1.15	3.54	0.14	0.861	0.003	Bal.
Double pass-307	0.32	0.50	1.55	4.10	0.16	0.989	0.003	Bal.
Single pass- 420	0.29	0.48	0.73	10.53	0.009	0.19	0.012	Bal.
Double pass - 420	0.32	0.50	0.75	10.68	0.011	0.19	0.012	Bal.

3.2. Microstructural changes

3.2.1. Base metal

Fig. 1 shows microstructure of the base metal in two different magnifications. The base metal microstructure contains tempered martensite and retained austenite. It is important to note that the Mo40 low-alloy steel is used in industry as a quench-tempered or normalize-tempered. In these cases, the microstructure of steel consists of tempered martensite or pearlite. As can be seen in Fig. 1a, the horizontal lines are related to the settlement of grains in the direction of the rolling process.

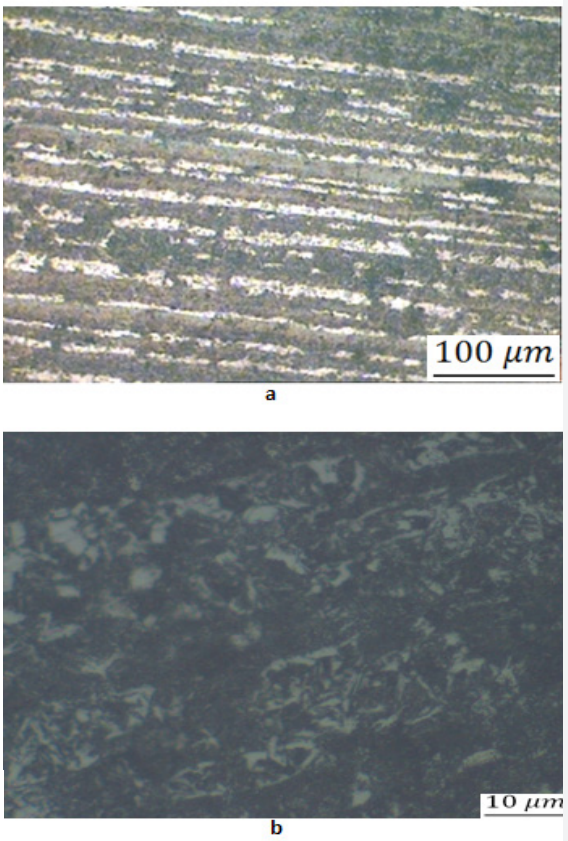

Fig. 1. Microstructure of the Mo40 low-alloy steel (a) tempered martensite with retained austenite (b) high-magnification (x750).

3.2.2. Overlay coating produced by the 307- flux core rod

The microstructures of the overlay coating fabricated by the flux core rod of 307 in single and double pass conditions are presented in Figs. 2 and 3. The microstructure of the overlay coating in the single pass condition (Fig. 2a) contains martensite with retained austenite and carbides. Fig. 2b depicts the carbide phases in high magnification. In addition, the microstructure of the coating in the double pass condition is displayed in Fig. 3 (a, b). The morphology of the coating in the double pass condition is observed to be the same as that in single pass condition. This means that the microstructure of the coating produced by the 307-flux core rod in both conditions is without any difference. The chemical composition only changes with increasing the number of passes which leads to alteration in the volume fraction of the phases. According to Table 6, the weight percent of carbon and chromium increases in the overlay coating of 307 in the double pass condition. In this regard, by comparison of Fig. 2 with Fig. 3, the changing of volume fraction of the phases is seen. These metallographic micrographs have a good agreement with the obtained results by

Mohammadikhah et al [14]. The SEM micrograph and the EDS analysis of the overlay coating of 307 produced by double pass are presented in Fig. 4. As can be seen from the EDS analysis, the identified carbide is the $(Fe, Cr)_{23}C_6$ with respect to the atomic weight of C,Cr, and Fe as well as the ratio of about 4 times of the (Fe, Cr) to the (C). Based on Fig. 5, the XRD analysis of the coating of 307 confirms the presence of martensite with retained austenite and the $(Fe, Cr)_{23}C_6$ carbide in the coating. This result is in good agreement with the obtained results from the EDS analysis.

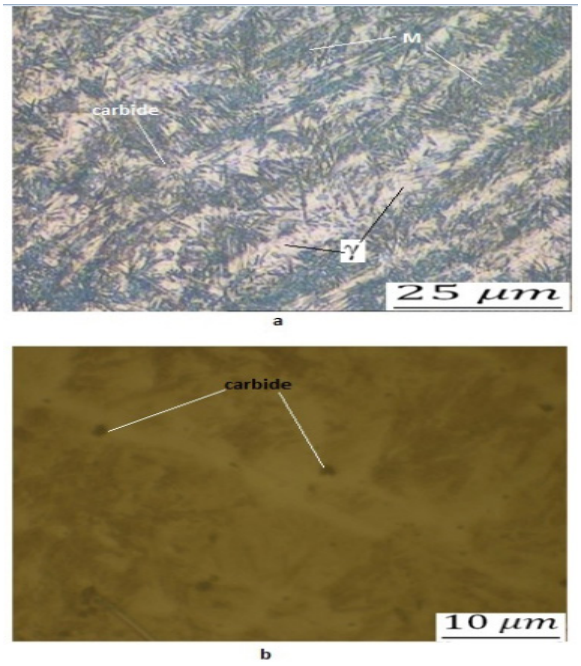

Fig. 2. OM morphologies of the coating of 307 produced by single pass (a) martensite with retained austenite and carbide (b) high- magnification view of the carbides (x750).

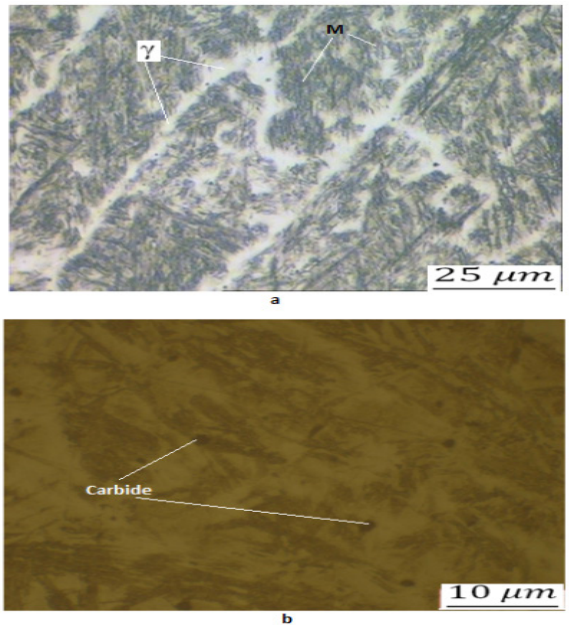

Fig. 3. OM morphologies of the coating of 307 produced by double pass (a) martensite with retained austenite and carbide (b) high- magnification view of the carbides (x750).

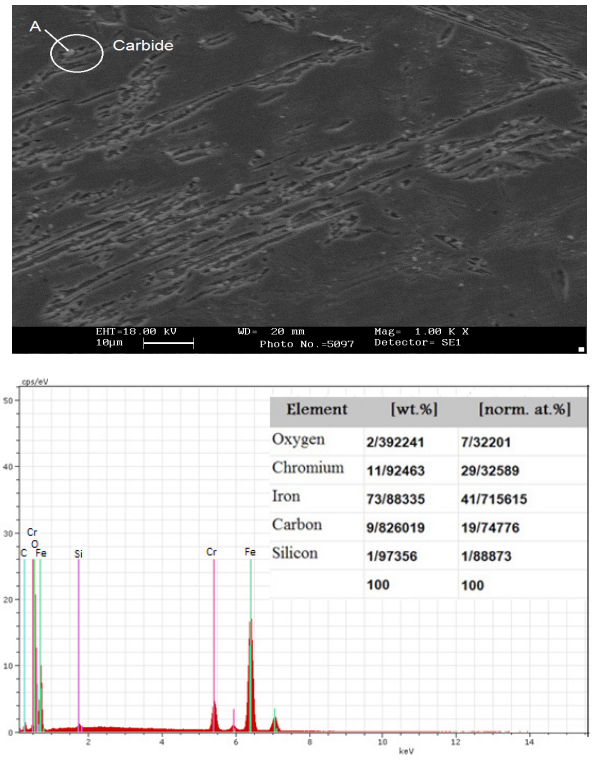

Fig. 4. SEM micrograph and the EDS spectra of the carbide phase (point A) in the coating of 307 produced by double pass.

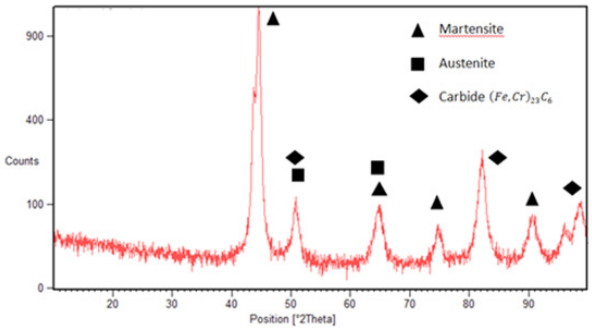

Fig. 5. XRD pattern of the coating of 307 produced by double pass.

3.2.3. Overlay coating produced by the 420- flux core rod

The microstructures of the overlay coatings fabricated by single and double pass are shown in Figs. 6(a, b) and 7(a, b), respectively. The microstructure of the coating in both conditions consists of martensite with retained austenite and carbide phases. The volume fraction of carbide in the coating of 420 increased as opposed to the coating of 307 due to the high weight percent of chromium. The SEM micrograph and the EDS analysis of the overlay coating of 420 produced by double pass are presented in Fig. 8. The analysis of point A (Fig. 8) is related to the $(Fe,Cr)_{23}C_6$ carbide.

In addition, the presented XRD analysis confirms the presence of martensite with retained austenite and the $(Fe,Cr)_{23}C_6$ carbide phases in the overlay coating microstructure (Fig. 9).

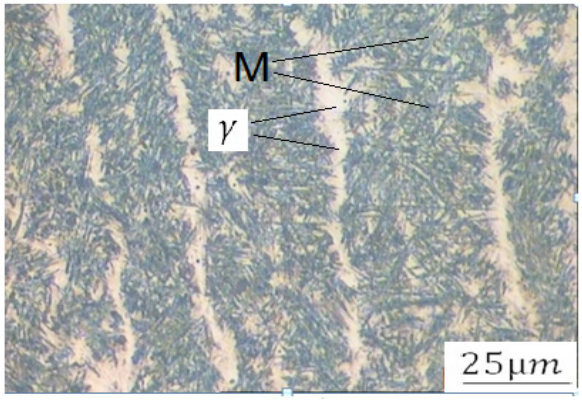

a

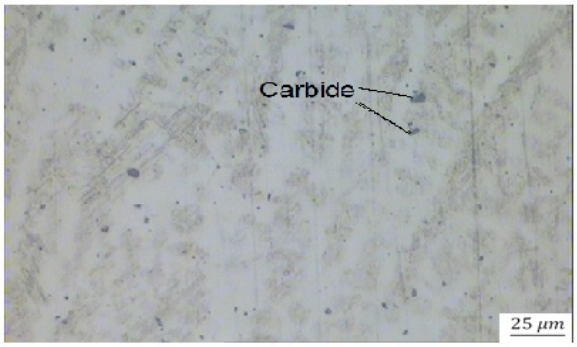

b

Fig. 6. OM morphologies of the coating of 420 produced by single pass (a) martensite with retained austenite (b) high- magnification view of carbides (x750), etched with nital in a shorter time.

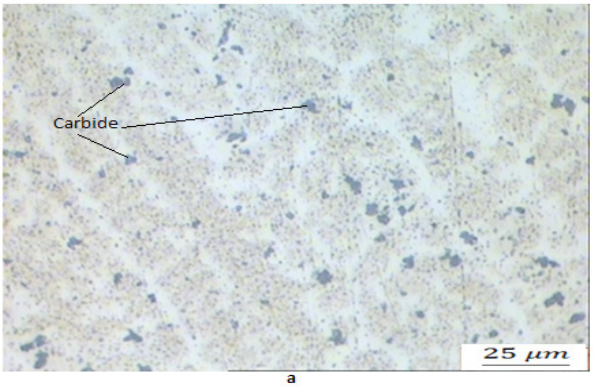

a

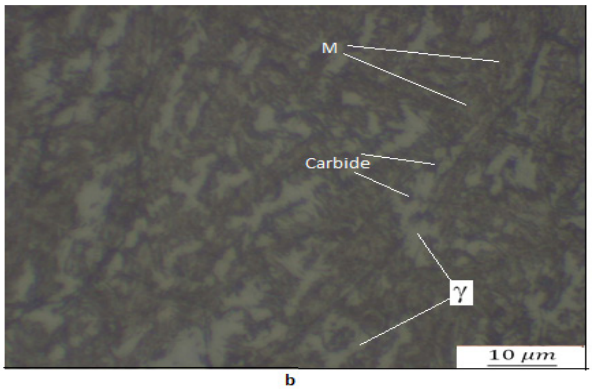

b

Fig. 7. OM morphologies of the coating of 420 produced by double pass (a) morphology of carbides, etched with nital in shorter time (b) microstructure of the coating (i.e. martensite with retained austenite and carbide), etched with nital in normal time.

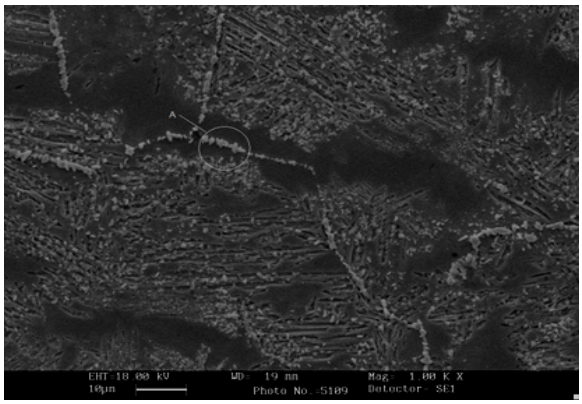

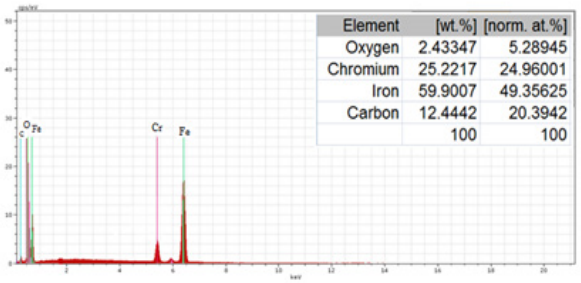

Fig. 8. SEM micrograph and the EDS spectra of the carbide phase (point A) in the coating of 420 produced by double pass.

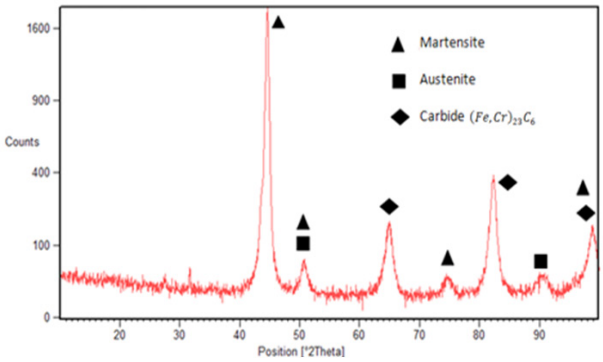

Fig. 9. XRD pattern of the coating of 420 produced by double pass.

3.2.4. Comparison of the coating microstructures

Based on the obtained metallography micrographs of the overlay coatings of 420 and 307, it is identified that the microstructure of coatings fabricated in both conditions is similar and they contain martensite with retained austenite and the $(Fe, Cr)_{23}C_6$ carbide. However, the volume fraction of the phases in the two coatings was different, so that this difference causes to change metallurgical and mechanical properties. The volume fractions of the phases are listed in Table 7.

The presence of the alloy elements such as chromium, molybdenum, manganese, and nickel influences the volume fraction of the phases. As can be seen from Table 7 that, the coating of 420 produced by double pass consists of high carbide and low austenite phases due to the presence of higher weight percent of

chromium compared to the other coatings. Additionally, due to the low weight percent of manganese and nickel as well as high weight percent of chromium, the austenite region and the amount of retained austenite decrease in the coating of 420 produced by double pass.

Table 7. Volume fraction of various phases on over coating.

Type of coating	Carbide $(Fe,Cr)_{23}C_6$	Remained Austenite	Martensite
Single pass-307	3	13	84
Double pass-307	6	15	79
Single pass-420	7	10	83
Double pass -420	11	12	77

3.3. Hardness results

The obtained results of hardness measurement on the surface of the coatings of 420 and 307 which are produced by single and double pass are arranged in Fig. 10. According to these results, it is clear that the lowering hardness (36 HRC) is related to the coating of 307 produced by single pass and the high hardness is determined for the coating of 420 produced by double pass. This is attributed to the high presence of the $(Fe,Cr)_{23}C_6$ carbide. As a result, the hardness increases with increasing of the volume fraction of the $(Fe,Cr)_{23}C_6$ carbide. The obtained results show that the increasing of hardness has a good agreement with the obtained results of other researchers due to the changing of the carbon content and increasing of the volume fraction of the $(Fe, Cr)_{23}C_6$ carbide [4]. In this respect, Mohammadikhah et.al [14] investigated the comparison of microstructure, hardness, and wear behavior of iron-based clad layer of plain steels with quench-tempered industrial steel and they concluded that the wear behavior of plain steels was increased with respect to the quench-tempered steels due to the high volume fraction of carbides.

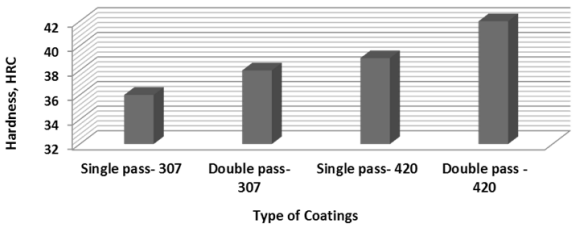

Fig. 10. Hardness profile of coatings.

3.4. Wear resistance

Generally, the wear resistance is related to the hardness of materials. According to Fig. 11, the amount of mass loss in the Mo40 steel specimen regularly and without showing the trekking behavior increases with increasing of the siling distance. These results are predictable according to the wear resistance behavior of the Mo40 low-alloy steel with hardness of 25 HRC. In addition, the wear resistance of the coating specimens is higher than that of the uncoated specimens. Due to the high hardness of chromium carbide, the formation of these carbides in the overlay coating can lead to reduction of damage caused by wear and abrasion. The chromium carbides decrease the amount of lost mass with reducing the depth of scratches and with their withdrawal. The obtained results from the effect of carbide on wear resistance are also examined by Buytoz et al. [13]. Accordingly, Jaffari et. al [15] studied on the resurfacing monoblock of wheels of the train wagons by submerge arc welding and they reported that the controlling of heating input can be affected on the changing dimensions and microstructure of wheels.

Therefore, it causes increasing of hardness and wear resistance. As can be seen in Fig. 11, the wear resistance of the coating of 420 produced by double pass is higher than that of the other overlay coatings. The overlay coating of 420 produced by single pass shows the same wear resistance. The high wear resistance in the coating of 420 is related to the high hardness of the overlay coating.

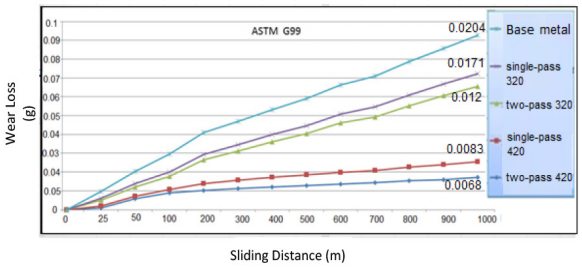

Fig. 11. Variation of wear loss versus the sliding distance under 130 N load at V = 0.05 m/s.

3.5. Wear mechanism

The investigation of Fig. 12 shows that the predominant wear mechanism of specimens is adhesive wear. The presence of the adhesive regions and particles on the surface can prove the adhesive wear mechanism.

As can be seen, the amount of adhesive wear in the overlay coating of 307 produced by double pass decreases compared to the base metal. Yang et al. [16] reported that the increasing of hardness on the surface leads to reduction of the adhesive wear. Therefore, the adhesive wear decreases in the coating of 307 produced by double pass with respect to the base metal

due to the increasing of hardness. Moreover, closer investigation of the worn-out surface and the EDS analysis on the overlay coating of 420 shows the presence of high oxygen on the adhesive region which is presented in Fig. 13. The presence of high oxygen in these regions is related to the increase of temperature during the wear testing [17]. Thus, the wear mechanism on the overlay coating consists of adhesive and tribochemical wear.

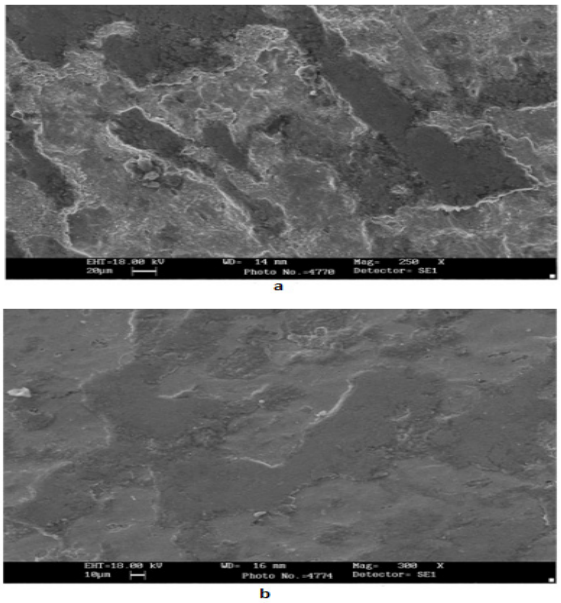

Fig. 12. SEM micrograph of the worn-out surface under 130 N load and 0.05 m/s sliding velocity after 1000 m sliding (a) base metal (b) coating of 307 produced by double pass.

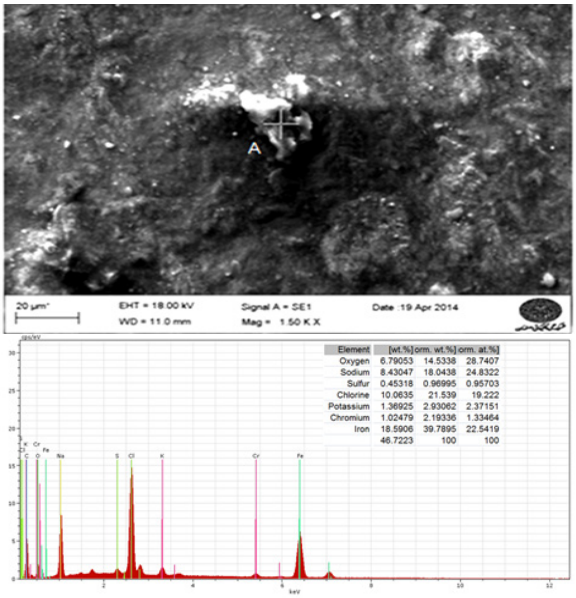

Fig. 13. SEM micrograph and the EDS spectra of the worn-out surface of the coating of 420 after the wear test.

4. Conclusion

- The chemical composition of the overlay coatings produced by double pass changes with respect to those produced by single pass. The presence of the carbon and chromium elements in hard surfaced specimen (as denoted by 307) produced by single and double passes increases from 0.28 to 0.32 and from 3.54 to 4.10, respectively. However, the presence of the chromium element in hard surfaced specimen (as denoted by 420) produced by single and double passes increases from 10.53 to 10.68.

- The microstructure of the overlay coatings of 307 and 420 produced by single and double pass contains martensite with retained austenite and the $(Fe,Cr)_{23}C_6$ carbide. The volume fraction of the $(Fe,Cr)_{23}C_6$ carbide in the coatings of 307 and 420 produced by single and double passes increases from 3 to 6 and from 7 to 11 percent, respectively. In contrast, the volume fraction of martensite in the coatings of 307 and 420 produced by single and double passes decreases from 84 to 79 and from 83 to 77 percent, respectively.

- The wear resistance in the coatings of 307 and 420 produced by double pass are higher than the coatings produced by single pass. In addition, the amount of average hardness in the coatings of 307 and 420 produced by single and double passes increases from 36 to 38 HRC and from 39 to 42 HRC, respectively.

- Adhesive wear was the dominant mechanism, but some degree of tribochemical wear was also observed.

References

[1] J.R. David, Surface Engineering for Corrosion and Wear Resistance. ASM International. Metals Park, Ohio, (2001).
[2] T. Hejwowski: Vacuum, 30 (2008), 5.
[3] D. K. Dwivedi : Mater. Sci. Technol , 10 (2004), 1326.
[4] C. Fan, M. Chen, C. M. Chang, W. Wu: Surf Coat Tech., 21 (2006), 908.
[5] S. Buytoz, M. Ulutan, M. M. Yildrim: Appl. Surf. Sci., 252 (2005), 1313.
[6] Y. C. Lin , J Mater Des.H. M. Chen: J Mater Des., 45 (2013), 6.
[7] Y. C. Lin, H. M. Chen: J Mater Des., 47 (2013), 828.
[8] L. Yuan-Ching, L. Yu-Chi: Surf Coat Tech., 205 (2011), 5400.
[9] S. Buytoz, M. Ulutan: Surf Coat Tech., 200 (2006), 3698.
[10] M. Soodi, S.H. Masoodi, M. Brandt: Adv Mat Res., 230-232 (2011), 949.
[11] V.Vukovic, R.Radic, S.Cudic: Metabk, 50 (2011), 133.
[12] ASTM G99-05, 2005, "Standard Test Method for Wear Testing with a Pin-on-Disk Apparatus", ASTM Book of Standards; Vol. 03.02, West Conshohocken, Pa, United States. In. (accessed).
[13] S. Buytoz: Surf Coat Tech., 200 (2006), 3734.
[14] M. Mohammadikhah, H. Sabet: Proc. of Steel Symposium, Yazd, Iran, (2012), 332.
[15] M. Jaffari, A. Ohadi, Proc. of 7th Conference of railway transportation, Iran, 2001.
[16] J. Yang, Z. Ye. Yong Liu, D. Yang and He. Shiyu: J Mater Des., 32 (2011), 808.
[17] H. Paydar, K. Amini, A. Akhbarizadeh: Kovove Mater., 52(2014), 163.